CFD pollution modelling and the influence on corrosive impact in blast stoves

J. Rieger[*]
Department of Environmental and Energy Process Engineering
Chair of Process Technology and Industrial Environmental Protection, Leoben, Austria
e−mail: johannes.rieger@unileoben.ac.at

C. Weiss
Department of Environmental and Energy Process Engineering
Chair of Process Technology and Industrial Environmental Protection, Leoben, Austria

B. Rummer,
voestalpine Stahl GmbH, Linz, Austria

ABSTRACT

The formation of nitrogen oxide NO during the combustion of enriched blast furnace gas in a blast stove at the voestalpine Stahl GmbH Linz is investigated.
The pollution formation is modelled with Computational Fluid Dynamics (CFD). The non-adiabatic numerical calculations investigate the turbulence-chemistry interaction in the combustion chamber using the Eddy Dissipation Concept in combination with a multi-step chemical reaction mechanism. Sub models are implemented to investigate turbulence of flow, radiative heat transport, flame characteristics and reaction kinetics of participating species in order to calculate the emission load in dependence on the operating conditions. The results confirmed the generally known trend that the NO emissions strongly depend on the temperature level of the stove dome. For the base operating point a NO emission load of about 25.1 mg/m$^3_{STP}$ (dry gas, 5 % reference oxygen) was calculated showing promising agreement with real plant data and literature trends.

Keywords: Combustion modelling, nitrogen oxides, hot blast stove

INTRODUCTION

Hot blast stoves (also called cowpers) are auxiliary installations in metallurgical plants being used to preheat the air for the blast furnace process. They consist of an upward flow burning and a downward flow regenerator shaft. A dome forms the horizontal connection between the shafts. Fig. 1 shows the geometry of a blast stove of the Blast Furnace A (BF A) at the voestalpine Stahl GmbH Linz with an overall height of approximately 45 m. The diameters of the burning shaft and the regenerator shaft are 4.8 m and 8.5 m respectively. The dome has a length of approximately 12 m.
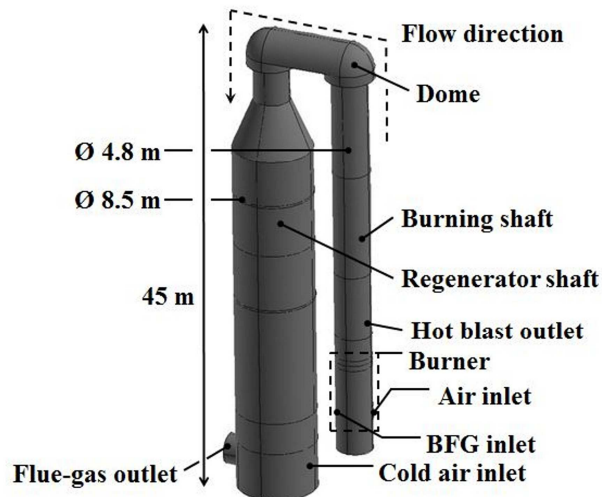
---

* Corresponding author

Figure 1. Blast stove geometry: Specification of flow direction and boundaries for the combustion air and fuel gas feed; BFG … Blast Furnace Gas

Four stoves operating on cyclical basis provide a continuous air supply of the BF A in Linz. The blast process consists of two main periods being interrupted by changeover periods (pressure swings). In the heating period (duration approximately 50 minutes) the stoves are heated up by burning gases (enriched blast furnace gas, BFG) until the dome is at the correct temperature (approximately 1300 °C to 1350 °C) [1]. The combustion starts in a ceramic burner at the bottom of the burning shaft. The flue gas streams upwards through the burning shaft and the dome into the regenerator shaft and subsequently in the direction towards the flue gas outlet at the bottom of the shaft. The shaft interior is composed of a refractory brickwork including vertical gas channels. The refractories come into contact with the flue gas and store the gas heat which is used for the preheating of cold air in the second period (blast period, duration ~ 40 min). Therefore combustion gas is cut off and by reversing the flow direction the stove is filled with compressed preheated air (5 to 6 bars absolute pressure and ~ 220 °C respectively) which enters the stove at the bottom of the regenerator shaft pressurizing the stove up to 5 bar (gauge pressure). The air passes the hot bricks by heating up to approximately 1350 °C [1]. Afterwards the so called hot blast leaves the stove via the hot blast outlet above the burner and is subsequently transported to the blast furnace.

NO_X triggered corrosive impact in blast stoves

Higher combustion temperatures in the stove lead to increased blast temperatures resulting in a reduced coke requirement for the iron production [1]. On the other hand higher temperature levels in the dome and the entire blast stove respectively enforce the formation of nitrogen oxides NO_X [2,3]. Control of emission is of great importance due to stringent legislation and furthermore in order to reduce corrosive impacts of the blast stove steel shell.

The formation of NO shows a strong dependence on the blast stove operating periods which was confirmed in several prior studies. Sucker et al. [3] announced that during the heating period NO formation preferentially takes place in the upper part of the burning shaft and the dome representing the high temperature combustion zone of the blast stove. Harp et al. [4] investigated the NO formation by means of mathematical model calculations. In the course of this study the influence of changing blast stove operating conditions was analyzed whereas Sucker's theory concerning the position of the NO formation maxima in the stove could be confirmed. Based on the numerical results Harp could generate operational measures to

reduce NO emissions e.g. a low offgas oxygen content and furthermore shorter changeover and blast air filling periods respectively lead to diminished reaction times for the NO formation whereas most of these measures are implemented in nowadays blast stove plants.

Under certain conditions pollutants such as nitrogen oxides are the starting point for severe stress corrosion cracking mechanism. During the air filling process of the stove after the heating period flue gas species e.g. NO diffuse through the slits of the refractory lining to the cold outer steel casing. Huijbregts et al. [5] found that this mass transfer occurs because of pressure swings being associated with load changes of the blast operation when switching from the heating period to the blast period. During the following blast period the flue gas cools down at the steel shell and NO is converted into NO_2 under presence of residual O_2. Nitric acid formed by NO_2 hydrolysis and sulfur oxides as a result of the fuel gas sulfur content increase the acid dew point of the entire combustion gas leading to the formation of aqueous condensates during the blast period as mentioned by Leferink et al. [6]. In further acid and sour gas reactions at the steel casing NO_3^- is partially reduced forming ammonia [4,5].

$$Fe \rightarrow Fe^{2+} + 2\ e^- \tag{1}$$

$$NO_3^- + 9\ H^+ + 8\ e^- \rightarrow 3\ H_2O + NH_3 \tag{2}$$

Eq. (1) represents the steel corrosion reaction and Eq. (2) the NH_3 formation respectively. Ammonia reacts with nitric acid and converts into ammonium nitrate (NH_4NO_3) showing strong stress corrosion cracking potential. This corrosion mechanism preferentially takes place in the lower section of the regenerator shaft (i.e. in the vicinity of flue gas outlet) especially in the welded areas of the steel shell being exposed to considerable tensile stresses [4,5].

In the present study Computational Fluid Dynamics (CFD) is used to investigate the pollution formation during the heating period (BFG combustion) in a blast stove of the voestalpine Stahl GmbH in Linz. The paper summarizes the calculated results concerning the NO and CO emission loads due to changing operating conditions such as gas and dome temperatures and air excess respectively. During the heating period both parameters influence the NO and CO concentration levels of the offgas considerably and therefore represent important blast process control values. The calculated emission loads can be used by the plant operators in Linz for a blast stove process control with respect to the legal NO_X and CO limits. In the subsequent sections the used models and assumptions for the simulation are described.

SETUP OF NUMERICAL METHODS

Since the blast stove possesses separate fuel gas and air supply channels the combustion gases do not mix until reaching the ceramic burner. Under these conditions a non-premixed combustion approach represents the basis for the species transport during the blast stove heating process.

Species transport

During BFG combustion chemical reactions with fast and slow kinetics and different reaction time scales are encountered. For a representative determination of pollution levels a simplified fast chemistry approach is not suitable. Therefore the Eddy Dissipation Concept (EDC) as based on the work of Magnussen and Hjertager [7] was applied for modelling of the turbulence-chemistry interaction. This model as an advanced development of Spalding's eddy

breakup theory [8] can be used to incorporate detailed non equilibrium chemical reaction kinetics. The conversion of species K is determined by solving the following transport equation

$$\frac{\partial}{\partial t}(\rho Y_K) + \frac{\partial}{\partial x_i}(\rho u_i Y_K) = \frac{\partial}{\partial x_i}\left(\rho D_K \frac{\partial Y_K}{\partial x_i}\right) + R_K \qquad (3)$$

consisting of a temporal change term (first part on the left hand side of Eq. 3), a convective term (second part on the left hand side) and a diffusive part (first term on the right hand side) respectively with Y_K and R_K denoting the mass fraction and the reaction rate of species K.

Since an explicit reaction transport equation per occurring species is implemented the EDC represents a good method to calculate the concentration of intermediate species being involved in pollution formation.

For description of the combustion kinetics a reaction mechanism of the system CH_4 / air provided by S. M. Correa [9] was used for the CFD calculations. This mechanism consists of 41 elementary reactions and the 16 following species, which are involved in the BFG combustion: N_2, O_2, CH_4, H_2, CO, CO_2, H_2O, OH, H, O, CH_3, HCO, HO_2, H_2O_2, CH_2O and CH_3O. The seven species at the beginning of the list are macro components. These components are addressed in the form of boundary conditions at the beginning of the CFD calculations specifying the feed composition. All the other species are considered as combustion intermediates and radicals. Prior CFD studies investigated the BFG combustion in the heating system of a coke oven using the Correa mechanism showed a good agreement between calculated and real plant NO and CO emission loads [10]. Therefore in this CFD study the above mentioned chemical reaction mechanism is considered to be adequate.

In the EDC the interaction of flow turbulence with combustion chemistry is managed by the assumption that chemical reaction occurs in small totally mixed regions, called turbulent structures or fine scales respectively (eddies). These regions are considered as ideal stirred vessels, where dissipation of turbulent kinetic energy takes place. Kinetic conversions as the rate controlling step are limited to this molecular mixed region. The length γ of the turbulent fine scales is determined according to [11] as

$$\gamma = \left(\frac{3\,C_{D2}}{4\,C^2_{D1}}\right)^{1/4}\left(\frac{\upsilon*\varepsilon}{k^2}\right)^{1/4} \qquad (4)$$

with C_{D1} = 0.134 and C_{D2} = 0.50 as model constants, $\upsilon*$ stands for the kinematic fluid viscosity in the turbulent structure given in m^2/s. Furthermore k and ε denote the turbulent kinetic energy in m^2/s^2 and the dissipation rate of the turbulent kinetic energy in m^2/s^3 respectively. These quantities will be explained in detail in the next section. The first part of Eq. (4) can be summarized as volume fraction constant being predefined in FLUENT as C_γ = 2.1377 [12]. The volume fraction of the flow occupied by the turbulent structures is modelled as γ^3. The estimated time scale τ for the mass transfer between the fine structures and the surroundings [11] is defined with following Eq. (5):

$$\tau = \left(\frac{C_{D2}}{3}\right)^{1/2}\left(\frac{\upsilon*}{\varepsilon}\right)^{1/2} \qquad (5)$$

The term $\left(\dfrac{C_{D2}}{3}\right)^{1/2}$ of Eq. (5) represents the time constant with a predefined value in FLUENT of 0.4082 [12]. The reaction rate R_K in Eq. (3) is determined as

$$R_K = \frac{\rho\,\gamma^2}{\tau\left(1-\gamma^3\right)}\left(Y_K - Y_K{}^0\right)$$

(6)

whereas Y_K denotes the mass fraction of species K in the fine structure zone after a reaction time τ and $Y_K{}^0$ stands for the species mass fraction in the surrounding fluid. The extent of R_K is limited to the mixing process and subsequently the amount of mass transfer between the fine structures and the surrounding fluid. A reactive fraction χ of the fine structures can be defined, where combustion takes place and energy is released, in the form [13]

$$\chi = \frac{\dfrac{\left((1+r_{fu})\cdot Y_\lambda\right)}{\overline{c}_{\mathrm{Pr}}}}{\dfrac{\overline{c}_{\mathrm{Pr}}}{(1+r_{fu})\cdot \overline{c}_{fu}}}$$

(7)

with $\overline{c}_{\mathrm{Pr}}$ and $\overline{c}_{fu}$ as mean local concentrations of reaction products and fuel respectively. Furthermore Y_λ denotes the mass fraction occupied by the turbulent structures and r_{fu} represents the stoichiometric oxygen demand. The definition of χ is used to model the fuel conversion and therewith the reaction rate R_K of the species transport equation (cf. Eq. 3) can be written in the following form

$$R_{fu} = \dot{m}\cdot \frac{\chi}{1-Y_\lambda}\cdot \overline{c}_{\min}$$

(8)

The reaction rate R_{fu} corresponds with R_K from Eq. (6) whereas $\overline{c}_{\min}$ denotes the smallest value of the local mean concentrations of fuel $\overline{c}_{fu}$ and oxygen $\overline{c}_{O2}$ respectively.

Turbulence
The changing operating conditions during the blast stove process (periodic change of hot and cold air, pressure swings and changes of flow direction) produce considerable unsteady conditions in the stove. A simplified quasi-steady state for the flow was used in FLUENT whereas the Reynolds-Averaged Navier-Stokes equations (RANS) for the conservation of mass, momentum, energy and species were implemented.

In the present study the k-ε model was considered to be accurate enough for turbulence description. This model solves two transport equations for the turbulent kinetic energy k and the dissipation rate ε of the turbulent kinetic energy in the following form [12, 14]

$$\frac{\partial}{\partial t}(\rho\,k) + \frac{\partial}{\partial x_i}(\rho\,u_i\,k) = \frac{\partial}{\partial x_j}\left[\left(\mu + \frac{\mu_T}{\sigma_k}\right)\frac{\partial k}{\partial x_j}\right] + G_k - \rho\varepsilon \qquad (9)$$

$$\frac{\partial}{\partial t}(\rho\,\varepsilon) + \frac{\partial}{\partial x_i}(\rho\,u_i\,\varepsilon) = \frac{\partial}{\partial x_j}\left[\left(\mu + \frac{\mu_T}{\sigma_\varepsilon}\right)\frac{\partial \varepsilon}{\partial x_j}\right] + \left(C_{1\varepsilon}\,G_k - C_{2\varepsilon}\,\rho\,\varepsilon\right)\frac{\varepsilon}{k} \qquad (10)$$

The dissipation means a conversion of kinetic energy into thermal energy (heat) leading to a decay of larger eddies into smaller. In Eq. (9) and (10) u_i represents the gas velocity, μ denotes the dynamic fluid viscosity, σ_k and σ_ε represent the turbulent Schmidt numbers and G_k represents the generation of turbulent kinetic energy due to mean velocity gradients. The model coefficients $C_{1\varepsilon}$ and $C_{2\varepsilon}$ denote standard FLUENT coefficients [12] and μ_T means the turbulent (eddy) viscosity being defined in the following form

$$\mu_T = \rho\,C_\mu\,\frac{k^2}{\varepsilon} \qquad (11)$$

with C_μ as a model constant. The locally available values for k and ε are used for the determination of the turbulent viscosity. The k-ε-model model is widely used for fully turbulent flows (high Reynolds numbers) with no swirling effects. During standard operating conditions in the blast stove the gas flow shows a Reynolds number $\mathrm{Re} = 1.7 \times 10^6$ representing a fully developed turbulent flow without recirculating regions and therefore justifying the choice of this turbulence model.

Radiation

Radiative heat transfer in the blast stove is of main importance since the majority of heat released during the combustion is transported to the walls via radiation. The optical thickness is a central criterion for the choice of the suitable radiation model. The combustion of BFG produces a transparent flame representing an optically thin medium. Therefore the heat exchange with adjacent walls of the combustion chamber has to be considered. Under this assumption the Discrete Transfer Radiation Model (DTRM) was chosen. The transferred heat is calculated during the simulation runs with the help of the following transport equation

$$\frac{dI}{ds} + a\,I = \frac{a\sigma T^4}{\pi} \qquad (12)$$

This approach is valid for optically thin media with no scattering effects [12] whereas I represents the radiant intensity directed along the pathway s of a ray beam. The coefficient a means the absorption coefficient of the fluid and is calculated by the weighted-sum-of-gray-gas-model approach (WSGGM) which is a standard FLUENT method. σ denotes the Stefan-Boltzmann constant.

The DTRM is a ray tracing model. In a preprocessing step a certain number of model beams is defined coming from each computational grid cell whereas the accuracy of the heat transfer calculation depends on the number of generated model beams. Several grid cells are summarized to face and volume clusters for CPU effort saving reasons. The length of the model beam pathways is calculated and the intercepted volume clusters are determined. These

information are stored in a separately file being used to calculate the transferred heat from the fluid to the combustion chamber walls by summing the change of intensity along the paths of each ray.

Pollution formation

The NO emission loads in this study consists of a thermal and a prompt fraction being calculated with standard FLUENT models. Prior simulations of the BFG combustion in the coke oven heating system proved that the standard models showed acceptable accuracy for the pollution modelling [10]. Therefore no additional sub models e.g. user defined functions were necessary. The thermal NO (Zeldovich mechanism) can be calculated as [14]

$$\frac{dNO_{therm}}{dt} = 2\,k\,[O][N_2] \tag{13}$$

where k denotes the rate constant for the formation reaction and the square brackets of O and N_2 represent the species concentrations in mol / m^3. The simplification of Eq. (13) originates from the short lifetime of N radicals being rapidly consumed in series reactions of the thermal NO mechanism. Therefore they can be neglected for the overall law in Eq. (13) due to the quasi-steady state assumption. The prompt NO (Fenimore mechanism) is determined as [12]

$$\frac{dNO_{prompt}}{dt} = k\,[O_2]^a\,[N_2][FUEL]\,e^{\frac{-E_A}{R\,T}} \tag{14}$$

whereas a represents the O_2 reaction order depending on the flame conditions [12]. The square brackets of O_2, N_2 and FUEL respectively denote the species concentrations in mol / m^3, E_A the activation energy in J / g mol, R the universal gas constant in J / K mol and T the temperature in K. CO and CH_4 are considered as the FUEL components in rate Eq. (14). All species in Eq. (7) and (8) have to be determined as macro and intermediate species concentrations and originate from the above mentioned 41-step combustion mechanism.

The following Eq. (15) to (17) show the thermal Zeldovich mechanism [14], which is the main NO formation path during BFG combustion.

$$N_2 + O \rightarrow NO + N \tag{15}$$

$$N + O_2 \rightarrow NO + O \tag{16}$$

$$N + OH \rightarrow NO + H \tag{17}$$
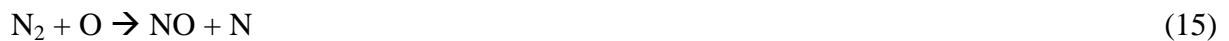
The O and H radicals generated in Eq. (16) and Eq. (17) interact in further reactions forming OH radicals. The modelling of CO oxidation in this study considers the two following elementary reactions in Eq. (18) and (19) describing the conversion of CO with O and OH radicals, which are part of the implemented Correa combustion mechanism [9].

$$CO + OH \rightarrow CO_2 + H \tag{18}$$

$$CO + O \rightarrow CO_2 \tag{19}$$
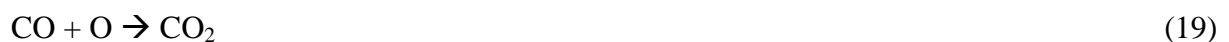
It can be seen from Eq. (15) to (19) that OH, O and H radicals play an important role in the pollution formation. The EDC model calculates the chemical reaction rates and therewith the local concentrations of the combustion intermediates by using the thermodynamic parameters

(e.g. activation energy) of the above mentioned 41 reaction Correa mechanism [9]. The impact of fluctuations caused by turbulence is considered since the local values of the turbulence parameters k and ε are used to calculate the reactive zones in the combustion regime and the mixing time scale respectively (cf. Eq. 4 and 5). In these zones O radicals are generated being subsequently used for the calculation of the NO reaction rate (cf. Eq. 13). The formation and conversion of the combustion intermediates is an important issue of this study and will be discussed in detail in the results section.

MODEL SETUP

The commercial software package FLUENT from ANSYS Inc. was used for the simulation runs, which are defined to be non-adiabatic since the energy equation has to be solved due to radiative heat exchange. The computational grid representing the control volume for the CFD runs was created with the software GAMBIT and consisted of 850000 tetrahedral cells. Because of the large construction height of the stove non-uniform cell spacing was applied whereas in the near burner region a finer grid with a typical cell size of ~ 15 cm was used and in the upper part of the burning shaft and the regenerator shaft respectively the cell size was ~ 30 cm. Complex geometries occur in the ceramic burner (several alternating gas channels for fuel gas and combustion air) and in the regenerator shaft (plurality of small-scale gas channels in the refractory bricks). A true to scale computational grid would lead to a large cell number and leading to non-economic simulation run times and a huge CPU effort respectively. Therefore simplified assumptions in the near burner region (only one supply channel per fuel gas and air flow) and in the regenerator shaft (refractory with fewer but larger scaled gas channels) were used. However the real surface ratios between fluid and solid domain of the large-scale plant were kept, which leads to realistic conditions with respect to shear forces, near-wall heat transfer and velocity distributions respectively justifying the above mentioned assumptions for the CFD calculations.

Boundary conditions

Apart from the dome the blast stove walls were assumed to be adiabatic. For the dome a constant temperature was predefined. In the course of a case study the dome temperature was varied. The emission factor for all walls was set to 0.8 (adequate for refractory materials). The gas inlet faces were defined as velocity inlets whereas the velocities were determined from the volume flow rates and the cross sectional areas. For the turbulence parameters a turbulence intensity of 10 % describing the ratio of the velocity fluctuations and the mean flow velocity was defined. Furthermore a hydraulic diameter of 0.61 m and 0.83 m for the fuel gas and the air inlet respectively were specified. For fully developed turbulent flames the turbulent intensity and the hydraulic diameter respectively are adequate turbulence parameters for the gas inlets [12]. In order to simulate the heat release from the flue gas to the refractory bricks an energy source term was defined for the fluid domain in the regenerator shaft transferring 125000 W/m^3 to the solid domain.

In the finite volume simulation runs the first order upwind scheme was used for discretization of the conservation equations of energy, momentum, k, ε and the species. Standard FLUENT convergence criteria have been used.

CASE STUDY

To investigate the influence of the operating conditions on the pollution formation during the heating period, a set of operating points specified by the voestalpine Stahl GmbH Linz was simulated. In the course of this study the combustion gas temperatures were varied leading to different temperature levels of the dome reaching from 1300 °C to 1380 °C. Furthermore the

effect of an air excess was investigated. To illustrate the numerical results one operating point represents the base case with a predefined dome temperature of 1300 °C. Table 1 and Table 2 show the fuel gas composition and the flow rates of the blast stove combustion gases. Fuel gas in this case means BFG which was enriched with natural gas in order to obtain a certain heating value needed for the hot blast generation. The combustion air consists of 78.40 $\%_{vol}$ N_2, 20.84 $\%_{vol}$ O_2 and 0.76 $\%_{vol}$ H_2O. The dome temperature in Table 2 represents the maximum reached value at the end of the heating period and the fuel gas and air temperatures respectively denote the values at the inlets.

Table 1. Composition of the blast stove fuel gas (BFG enriched with natural gas)

CH_4 $\%_{vol}$	CO $\%_{vol}$	H_2 $\%_{vol}$	H_2O $\%_{vol}$	CO_2 $\%_{vol}$	N_2 $\%_{vol}$	Lower heat value (MJ/m^3_{STP})
0.06	22.90	6.32	2.05	22.07	46.60	3.4

Table 2. Fuel gas (FG) and air boundary conditions for the base operating point

Flow rates (m^3_{STP}/h)		Gas velocities (m/s)		Temperatures (°C)		
FG	AIR	v_{FG}	v_{AIR}	T_{FG}	T_{AIR}	T_{Dome}
146952	117363	55.71	67.19	19.5	190.3	1300

SIMULATION RESULTS

Figure 2 shows the simulated flow profile in the near burner region of the blast stove in terms of velocity vectors (Figure 2 a) and pathlines (Figure 2 b). It is obvious that the geometry of the gas supply channels showing an inclination and a trapezoidal channel widening in flow direction influences the flow profile. A ceramic grate with a height of 0.5 m is placed above the burner for reasons of flow homogenization which can be seen in Figure 2 b. However the main part of the combustion gases moves upwards along the walls after entering the burner leading to a non-symmetric flow profile in the bottom region of the burning shaft (cf. Figure 2 a). Further upstream at a height level of ~ 30 m (which is not seen in Figure 2) the flow is more or less homogenized and distributed all over the cross sectional area.

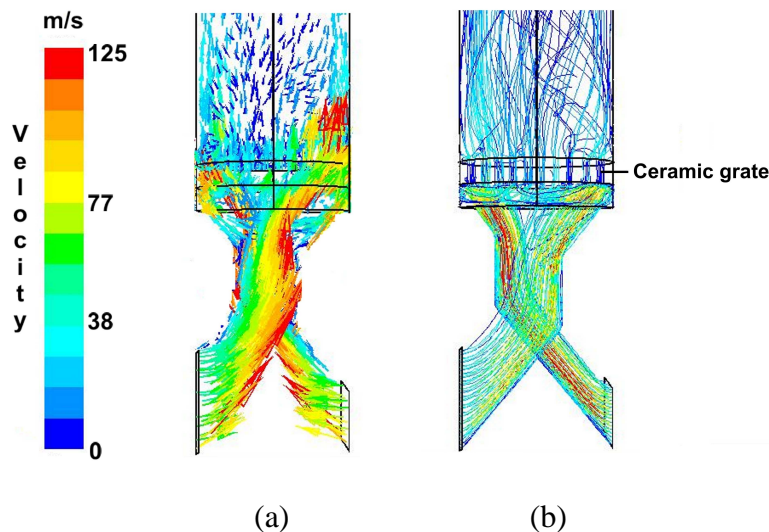(a)   (b)

Figure 2. Calculated flow profile in the near burner region during BFG combustion for the base operating point expressed as velocity vectors (a) and velocity pathlines (b)

The simulated gas temperature distribution in the stove can be seen in Figure 3 correlating with the flow profile (cf. Figure 2). The non-uniform gas flow in the burning shaft induces increased shear rates in the near wall region leading to an enhanced mixing of fuel gas and combustion air. As a consequence the combustion reaction and the energy release start at the walls which can be seen in Figure 3 due to the raised temperatures occurring in this region. Further upstream the flow and as a consequence the temperature profile homogenize. The stove's peak temperature occurs in the dome and the beginning of the regenerator shaft showing a constant absolute level in this area which was set in the form of a wall boundary condition before the start of CFD calculations. At the beginning of the regenerator shaft an uneven distributed flow exists. The dome deflects the gas flow, which can be seen due to the non-uniform temperature distribution in the regenerator shaft (cf. Figure 3 b). Further downstream the flue gas temperature decreases towards the gas outlet due to heat absorption by the refractory bricks leading to a final flue gas temperature of ~ 600 K.
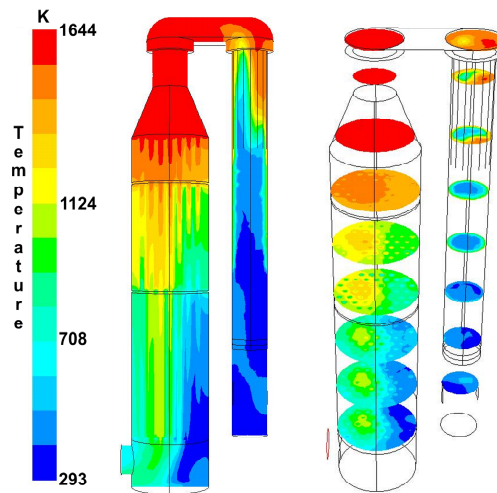

Figure 3. Calculated gas temperature profile in the blast stove during BFG combustion for the base operating point

It is generally known that the temperature has an important influence on the formation of NO during combustion processes which can be seen in Figure 4 indicating the calculated NO distribution in the blast stove. The simulation runs estimated the share of thermal NO in total NO emissions with ~ 90 % whereas the peak concentration occurs at the beginning of the regenerator shaft (cf. Figure 4 a). The remaining 10 % are prompt NO. The NO formation mainly takes place in the upper part of the burning shaft and the dome respectively until the beginning of the regenerator shaft (cf. Figure 4 b) representing the hottest area in the stove. This correlates with the simulated temperature profile (cf. Figure 3) and aligns with literature trends as well [3]. In the downflow regenerator shaft the NO formation stops due to the reduced gas temperatures leading to a NO exit concentration of 22 ppm (= 25 mg/m$^3_{STP}$, dry gas, 5 % reference O_2) for the base operating point.
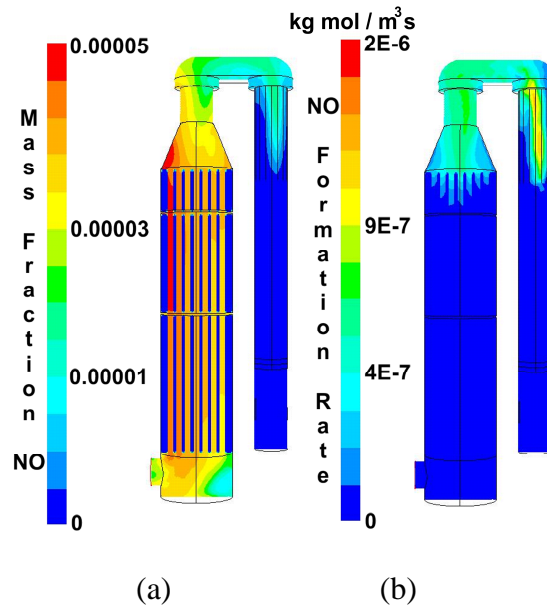
Figure 4. Calculated NO distribution in the blast stove during BFG combustion for the base operating point expressed as mass fraction (a) and NO formation rate (b)
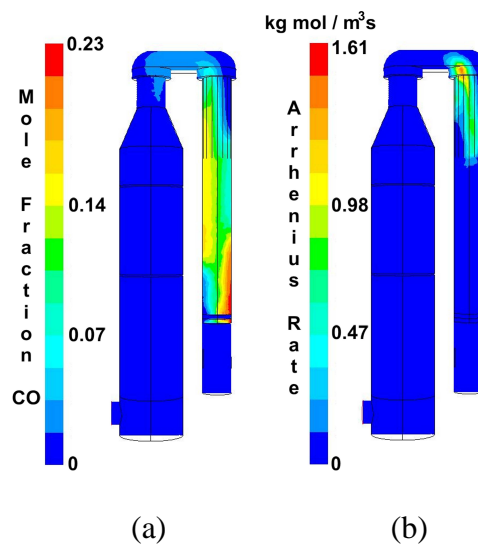

Figure 5. Calculated molar fraction of CO (a) and the CO oxidation rate (b) in the blast stove during BFG combustion for the base operating point

The simulated CO distribution can be seen in Figure 5. The fuel gas, which enters the burning shaft, contains 22.9 %$_{vol}$ CO (cf. Table 1). In the near burner region CO moves upwards along the wall due to the inclined gas flow in this region (cf. Figure 5 a). In the upper part CO is oxidized via Eq. (12) and Eq. (13) [9].

The CO oxidation rate of Eq. (12) is shown in Figure 5 b. The CO burnout starts in the upper burning shaft whereas the local maximum can be found at the beginning of the dome. The CO oxidation via Equ. (13), which is not seen in Figure 5, starts in the same region as well and is continued until the end of the dome. The entire CO oxidation region corresponds with the high temperature zone of the blast stove (cf. Figure 3) resulting in a flue gas exit CO

concentration for the base operating point of ~ 27 ppm (= 28 mg/m$^3_{STP}$, dry gas, 5 % reference O$_2$).
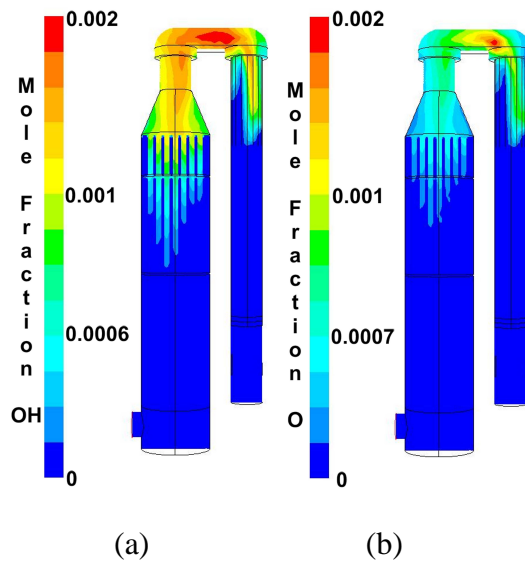

(a)   (b)

Figure 6. Calculated molar fraction of OH (a) and O (b) for the base case BFG combustion

Figure 6 points out the simulated molar distributions of OH and O in the blast stove. It is generally known that radical formation is enhanced at higher temperatures. Figure 6 proves this fact showing the maximum OH and O formation in the upper burning shaft and the dome representing the high temperature zone during the heating period as already mentioned whereas the OH and O profiles show strong similarities.

The simulation runs showed a contrary effect concerning the temperature dependence of NO and CO emission loads during the BFG combustion. This behaviour was also a subject of investigation in previous studies [10]. Enhanced NO formation and CO burnout preferentially proceed faster with increasing temperature levels. This can be clearly seen when comparing the calculated temperature profile (cf. Figure 3) with the NO and CO distribution (cf. Figure 4 and 5 respectively). The peak temperatures in the upper burning shaft and the dome lead to a maximum NO formation and CO oxidation rate in this area. On the other hand decreasing temperature levels result in a diminished NO formation and higher CO emissions. The radical profiles of OH and O give a reasonable explanation for this phenomenon. Following from Eq. (9) to (13) it is obvious that NO formation and CO oxidation are strongly connected with the radical pool in the blast stove. Increased OH and O concentrations (cf. Figure 6 a and 6 b) in the upper burning shaft and the dome respectively lead to a stronger NO formation rate (cf. Fig. 4 b) and a better CO burnout (cf. Fig. 5 b).

Figure 7 shows the NO emissions (in ppm, wet gas, no oxygen reference) in dependence of the dome temperature comparing calculated CFD data with literature data [2] and real plant emission loads. The dome temperature is the maximum reached value at the end of the heating period. The cloud of measured values represents the standard operation of the blast stove plant at the voestalpine Stahl GmbH Linz with a dome temperature of ~ 1300 °C. It can be clearly seen that the calculated and real plant data show good agreement. Furthermore the generally known trend from literature that NO emission increases with rising dome temperature was proved by the CFD model.

Historically blast stoves were operated at higher temperature levels with dome temperatures up to 1500 °C leading to a raised process efficiency i.e. increased hot blast temperatures lead to a reduced coke consumption for iron production in the blast furnace. Nowadays beside the stress corrosion cracking mechanism discussed above, plant operators have to face stringent legislation. Therefore dome temperatures have to be reduced due to legal NO_X limits. CFD calculations showed that a dome temperature of > 1350 °C must be considered as too high for staying below the legal NO_X limit, which is set to 80 mg/m^3_{STP} (dry gas, 3 % reference O_2) for the blast stove plant Linz.
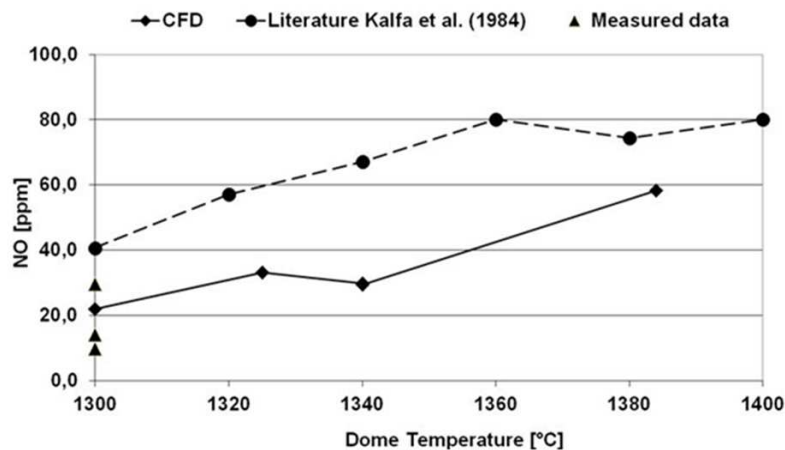

Figure 7. NO emissions depending on the dome tempterature during BFG combustion; Solid line: CFD data; Dashed-line: Literature data; Triangles: Measured data

CONCLUSION

In the current study Computational Fluid Dynamics (CFD) was used to investigate the pollution formation in a blast stove at the voestalpine Stahl GmbH Linz during the combustion of Blast Furnace Gas (BFG). Therefore non adiabatic simulation runs using the commercial software package FLUENT from ANSYS Inc. were targeted on the influence of operating conditions on NO and CO emission loads during the heating period. In the course of this study a set of 5 operating points was investigated whereas the dome temperature and the temperatures of fuel gas and combustion air respectively and furthermore the air excess were varied. The Eddy Dissipation Concept (EDC) was used for the turbulence-chemistry interaction in combination with a CH_4 combustion mechanism in order to consider reaction kinetics of intermediate combustion species.

CFD results confirmed the generally known trend that NO emissions increase with rising dome temperature level representing an important blast stove process value whereas good agreement with real plant emission data of the blast stove plant in Linz could be achieved. In addition an increased air excess when raising the residual O_2 content in the flue gas from 1 %$_{vol}$ (representing the standard operation with an air excess ratio λ of 1.19) up to 2 %$_{vol}$ ($\lambda = 2.12$) leads to an insignificantly NO reduction.

A contrary effect between NO and CO emissions was confirmed. Intermediate species (radicals) such as O, H and OH play an important role during formation and conversion of NO and CO whereas during the heating period NO formation and CO oxidation preferentially take place in the upper burning shaft and the dome representing the high temperature zones. The importance of intermediate species reaction kinetics justifies the utilization of the CPU

intensive EDC in the current study for detailed determination of the species concentration levels.

The numerical results confirmed generally known trends concerning emission loads in dependence on the blast stove operating conditions. Furthermore scientific knowledge could be gained concerning the connection between pollution formation and the combustion intermediate chemistry during BFG combustion. Plant operators can use the information of the present manuscript to optimize blast process operating conditions (e.g. temperature level, gas feed) with respect to legal limits.

Considering a refined heat transfer modelling between the gas flow and the refractory brick in the regenerator shaft as well as a CFD study of the NO formation during the blast period remain as open challenge for future investigations.

REFERENCES

1. Iron and Steel Production, *Best Available Techniques (BAT) Reference Document*, Institute for Prospective Technological Studies, European IPPC Bureau, Seville, Spain, 2012.
2. Kalfa, H., Bühler, H. E., Interkristalline Spannungsrißkorrosion an Hochtemperatur-Winderhitzern, *Chem.-Ing.-Tech.*, Vol. 56, No. 84, pp 23-31, 1984.
3. Sucker, D., Harp, G., Dorweiler, W., Kondensate und Gasatmosphäre in Winderhitzersystemen in Zusammenhang mit der interkristallinen Spannungsrißkorrosion, *Stahl und Eisen*, Vol. 101, No. 15, pp 25-31, 1981.
4. Harp, G., Klima, R. D., Sucker, D., Einfluß betrieblicher Maßnahmen auf die Bildung korrosiver Kondensate beim Winderhitzerbetrieb, *Stahl und Eisen*, Vol. 110, No. 6, pp 121-127, 1990.
5. Huijbregts, W. M. M., Leferink, R. G. I., Latest advances in the understanding of acid dew point corrosion: corrosion and stress cracking in combustion gas condensates, *Anti-Corrosion Methods and Materials*, Vol. 49, No. 2, pp 118-126, 2002.
6. Leferink, R. G. I., Huijbregts, W. M. M., Nitrate stress corrosion cracking in waste heat recovery boilers, *Anti-Corrosion Methods and Materials*, Vol. 51, No. 3, pp 173-188, 2004.
7. Magnussen, B. F., Hjertager, B. H., On mathematical modeling of turbulent combustion with special emphasis on soot formation and combustion, *Symposium (International) on Combustion / The Combustion Institute*, Vol. 16, No. 1, pp 719-729, 1977.
8. Spalding, D. B., Mixing and chemical reaction in steady confined turbulent flames, *Symposium (International) on Combustion / The Combustion Institute*, Vol. 13, No. 1, pp 649-657, 1970.
9. Yang, B., Pope, S. B., An Investigation of the Accuracy of Manifold Methods and Splitting Schemes in the Computational Implementation of Combustion Chemistry, *Combustion and Flame*, Vol. 112, No. 1, pp 16-32.
10. Weiss, C., Rieger, J., Rummer, B., Formation and Control of Nitrogen Oxide NO in the Heating System of a Coke Oven, *Environmental Engineering and Science*, Vol. 29, No. 7, pp 555-562, 2012.
11. Gran, I. R., Magnussen, B. F., A Numerical study of a bluff-body stabilized diffusion flame - Part 2: Influence of combustion modeling and finite-rate chemistry, *Combustion Science and Technology*, Vol. 19, No. 1-6, pp 191-217, 1996.
12. FLUENT User Guide, ANSYS Inc., 2006.
13. Magnussen, B., F., On the structure of turbulence and a generalized eddy dissipation concept for chemical reaction in turbulent flow. 19th American institute of aeronautics and astronautics aerospace science meeting, 1981.

14. Warnatz, J., Maas, U., Dibble, R. W., *Verbrennung - Physikalische Grundlagen, Modellierung und Simulation, Experimente, Schadstoffentstehung*, 3rd Edition, Springer Verlag Berlin-Heidelberg, 2001.